Dutta, T., Medina Bailon, C., Rezaei, A., Nagy, D., Adamu-Lema, F., Xeni, N., Abourrig, Y., Kumar, N., Georgiev, V. and Asenov, A. (2021) TCAD Simulation of Novel Semiconductor Devices. In: International Conference on ASIC (ASICON) 2021, Kunming, China, 26-29 October 2021, ISBN 9781665438674

(doi: 10.1109/ASICON52560.2021.9620465)

This is the Author Accepted Manuscript.

There may be differences between this version and the published version. You are advised to consult the publisher's version if you wish to cite from it.

http://eprints.gla.ac.uk/258912/

Deposited on: 15 November 2021

TCAD Simulation of Novel Semiconductor Devices

Tapas Dutta, Cristina Medina-Bailon, Ali Rezaei, Daniel Nagy, Fikru Adamu-Lema,
Nikolas Xeni, Yassine Abourrig, Naveen Kumar, Vihar P. Georgiev, and Asen Asenov

Device Modelling Group, School of Engineering, University of Glasgow
Glasgow G128LT, Scotland, UK.
tapas.dutta@glasgow.ac.uk, vihar.georgiev@glasgow.ac.uk

Abstract—**Simulation of conventional and emerging electronic devices using Technology Computer Aided Design (TCAD) tools has been an essential part of the semiconductor industry as well as academic research. Computational efficiency and accuracy of the numerical modeling are the key criteria on which quality and usefulness of a TCAD tool are ascertained. Further, the ability of the tools to incorporate different modeling paradigms and to be applicable to a wide range of device architectures and operating conditions is essential. In this paper, we provide an overview of the new device simulator NESS (Nano-Electronic Software Simulator) developed at the University of Glasgow's Device Modelling Group. It is a fast and modular TCAD tool with flexible architecture and structure generation capabilities, and contains different modules including classical, semi-classical, and quantum transport solvers, mobility calculation, kinetic Monte-Carlo and others. NESS can also take into account various sources of statistical variability in nanodevices and can perform simulations of thousands of microscopically different devices created by the structure generator. This state-of-the-art tool is designed to be open source and is being made available to the device engineering community at large for active collaboration and development.**

Keywords—TCAD, Variability, Drift-Diffusion, Quantum Correction, Kubo-Greenwood, Non-Equilibrium Green's Function, Kinetic Monte-Carlo

I. Introduction

TCAD tools play important roles for the semiconductor device industry including in-depth understanding the underlying physics of device operation, device optimization reducing costly wafer reruns in the foundry, debugging fabrication faults, exploring and isolating the impact of different process and statistical variability sources, and performance analysis of novel devices prior to fabrication using DTCO (Device Technology Co-Optimization) techniques. While there exist mature commercial TCAD tools, they have limitation with regard to quick deployment of new physical models and simulation techniques needed for the simulation of future semiconductor device candidates. In contrast, open source tools like NESS [1]–[5], allows easy collaboration and on-demand addition of new modules and numerical algorithms, thus enabling faster development of full-fledged simulators for emerging devices. Further, an open-source software presents a great opportunity for teaching semiconductor device physics as well as the implementation details of the numerical methods applied to solve the different equations.

In Section II, we explain the structure of NESS consisting of the input and output features, and the communication between different modules. In Section III, we summarize the structure generator and physical models incorporated into the tool. In Section IV we highlight the capabilities of NESS by presenting results from simulation of novel semiconductor devices, concluding the paper in section V.

II. NESS: Tool Overview

The flowchart in Fig. 1 shows the overall organization of NESS. The device structures are created by the structure generator. The effective mass extractor module yields the effective masses in different valleys from first principle and tight binding simulations, and injects this information in the material database which additionally contains all the necessary material and model parameters needed for running NESS. The key modules in NESS: the Poisson, Schrödinger, and k.p solvers are shared among the other modules e.g. 3D drift-diffusion (with quantum corrections) and NEGF formalism, mobility calculation using Kubo-Greenwood method, a module for gate tunneling leakage, a kinetic Monte Carlo module, and a module for Negative Capacitance FETs. The modules in NESS incorporate a high degree of parallelism using MPI and OpenMP approaches. The output data from the simulations are stored in VTK format as well as text files.
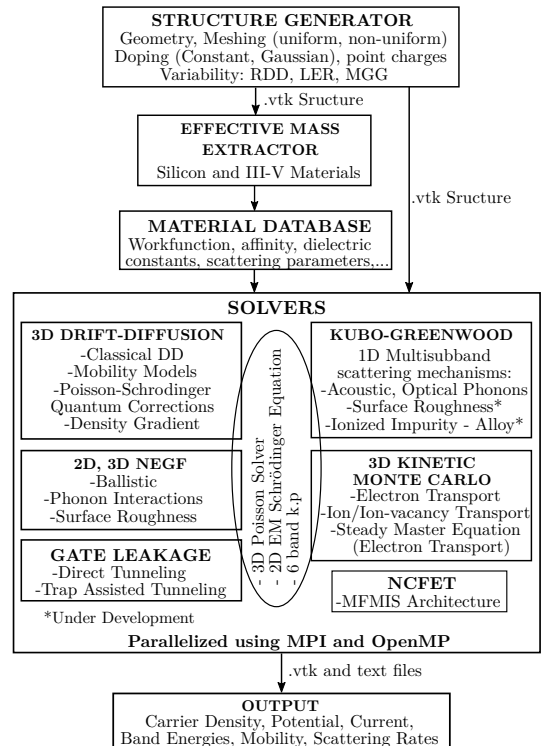

Fig. 1. NESS in a nutshell: Flowchart showing different modules and how they are linked.

III. Different Modules of NESS

A. Structure Generator

The structure generator (SG) is one of the most important parts of NESS which creates the input device structure as per user specifications. Users can generate all conventional and

advanced device structures using SG. For example, silicon-on-insulator (SOI), stacked nanowire and bulk MOSFET architectures are some of the few presented in Fig. 2. SG has three main components. The first is an input data management section where information about material types, specific commands to create individual geometric parts, details about doping scheme, meshing and configuration orders are all listed to create the intended device structure and the corresponding simulation domain.

The second part is the Structure Generator Engine where primitive geometrical objects, like cuboid, ellipse and cylinder are created and these individual geometries (boxes) are configured to form the final device structure that the users want to simulate. In the structure generator engine, doping can be added as required to the particular regions of interest. Users can choose between uniform or Gaussian type doping profiles. The main variability effects like random discrete dopants (RDD), metal gate granularity (MGG) or line edge roughness (LER) can also be introduced and configured in the structure generator engine section. Furthermore, users can also define point charges create mesh, and define contacts in this section. The third component of SG is the assembly of all the primitive geometric boxes, including all the material information and writing the complete device structure to a file that is readable by NESS. Currently NESS-SG output format is VTK (Visualization Toolkit). The data set is a rectilinear grid type where the geometric boxes are defined with (x, y, z) coordinates.
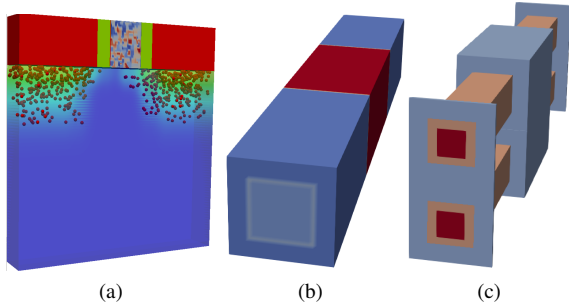

Fig. 2. Examples of different device structures generated using the SG module: (a) Bulk MOSFET with variability effects introduced (b) Single NWFET, (c) Stacked NWFET.

B. Effective Mass Extractor

Effective masses are some of the most important parameters needed in a semiconductor device simulation. An effective mass extractor module (EME) has been implemented in NESS, that can be used for both Silicon, Germanium, III-V, and indeed any other semiconductor material. First the bandstructure is calculated using an external first principle, tight binding or other material modeling. The EME module then extracts the transport effective mass, from the curvature of the bands from the bandstructure output under parabolic assumption. The confinement effective mass is calculated by equating the difference between the two lowest subband energies obtained from solution of the Schrödinger's equation and the quantization energy obtained from the bandstructure calculation. Details can be found in [6]. In Fig. 3, we have shown that a good agreement can be found for the minima and curvature at the minima for the bandstructures obtained from tight-binding calculation using the QuantumATK tool [7] and the parabolic band structures calculated using the results from the EME.
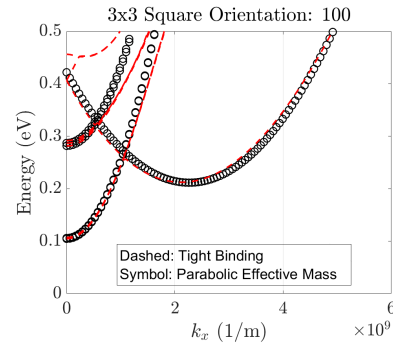

Fig. 3. Comparison of the electronic band structure calculated using tight binding and the Parabolic Effective Mass approximation using the EME module for a 3nm×3nm square Nanowire with orientation along 100 direction. The extracted effective masses are: Δx: m_x=0.932, m_y=0.267, m_z=0.267; Δy: m_x=0.257, m_y=0.678, m_z=0.305; Δz: m_x=0.257, m_y=0.305, m_z=0.663.

C. Classical and Quantum-Corrected Drift-Diffusion Module

NESS contains a classical three-dimensional drift-diffusion simulator module including mobility models taking into account the impact of doping and electric fields. Two approaches for Quantum correction have been implemented - first, based on the solution of 2D Schrödinger equation in planes normal to transport (details in [8]), and second, based on the solution of the 3D density gradient (DG) equation [9]. Either of these approaches yields a quantum carrier density profile which is used to calculate a quantum correction term which modifies the electrostatic potential in the device, which is further used as the driving force for the carrier continuity equation, the output of which is the quantum-corrected carrier density.

D. Non-equilibrium Green's Functions (NEGF) Module

The NEGF formalism is a widely applied framework for analyzing the quantum transport in mesoscopic and nanoscale devices, capturing quantum phenomena such as confinement, tunneling, coherence, and particle-particle interactions. The charge density, potential profile, and the current flow in the system are obtained by performing a self-consistent solution of the Poisson equation and the NEGF transport equations. The NEGF formalism in NESS includes both ballistic transport and scattering including currently acoustic- and/or optical-phonon scattering, which enables electron-phonon (e–ph) interactions [10] within the self-consistent Born approximation (SCBA) [2], [4]. The electron NEGF module is based on an effective mass Hamiltonian and the hole NEGF module is based on a *k.p* Hamiltonian.

E. Kubo-Greenwood Module

The Kubo-Greenwood (KG) approach for solving the Boltzmann Transport Equation in combination with the Matthiessen rule provides accurate low-field electron mobility in the low-field limit, with significantly reduced computational cost compared to full-scale simulations (such as Monte Carlo or NEGF). The KG formalism implemented in NESS is based on the long-channel approximation for the calculation of the low field mobility in relaxation time approximation [11]. Moreover, this model have been already compared against the one-dimensional ensemble Monte Carlo (1DMC) simulator [4] and literature to show its accuracy. Currently, the acoustic and optical phonon scattering mechanisms are included in NESS,

the surface roughness mechanism is in a testing stage, and ionized impurity and alloy scattering mechanisms are under development.

F. Kinetic Monte Carlo Module

The Kinetic Monte Carlo (KMC) module in NESS is designed to capture mesoscopic phenomena in nanoscale devices including degradation, noise, trap assisted tunnelling, resistive and phase change memory effects. It includes self-consistent iterations between the Poisson equation and the KMC engine. The KMC engine calculates the stochastic time steps between the transitions in the mesoscopic system based on the probability of all mesoscopic transitions including trapping and de-trapping, hoping, tunnelling, ion and vacancies movements etc and selects the transition mechanism after the stochastically selected waiting time.

IV. NOVEL DEVICE SIMULATION USING NESS

A. Nanowire FETs

Nanowire FETs (NFETs) are poised to replace the FinFETs at 3nm CMOS and beyond. NFETs can be simulated in NESS using the classical DD, Poisson-Schrödinger based DD, DG based DD, and the NEGF modules. The DG module can be calibrated to reproduce quantum confinement results and measurement data. A comparison of the carrier density profile and transfer characteristics for a 3nm $\times$ 3nm square NWFET obtained from classical DD and density gradient corrected DD is shown in Fig. 4 for different DG masses in the confinement direction. The DG approach is able to reproduce realistically the quantum charge profile with maximum carrier density at the center of the nanowire, and the corresponding threshold voltage shift in the I-V characteristics due to quantum confinement.
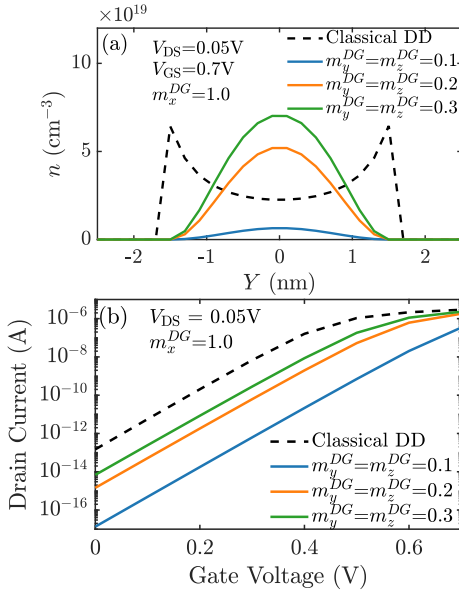

Fig. 4. Comparison of (a) electron density along the confinement direction, and (b) transfer characteristics for a square NWFET (L_g=10nm, t_{ox}=1 nm) using classical DD and DG formalisms showing the effect of the transverse DG mass with fixed longitudinal DG mass.

B. Resonant Tunneling Diodes (RTDs) with RDDs

Owing to the ultrahigh frequency capabilities and relatively simple structure, the RTDs are very promising candidates for wireless and optical resonant THz frequency generation and detection. Here, we illustrate the NESS capabilities in a purely ballistic numerical investigation of the important role of the RDD variability using the NEGF module in a double barrier GaAs-Al$_x$Ga$_{1-x}$As RTD device with a square cross-section (10nm$\times$10nm) and a total length of 55nm implemented in the nanowire structure shown in Figure 5(a). We have carried out simulations considering a sample of 10 devices with unique positions of the RDDs to investigate their impact on the resonance voltage. Comparing their I-V curves with the smooth (without any RDDs) RTD, we see that there is a direct link between the number and positions of the RDDs, and the position of the resonance peak, valley, and magnitude of the simulated current (see Figure 5(b)) which verifies that the quantum nature of the resonance condition can be significantly altered due to the RDDs [5]. Therefore NESS can be used to predict and tailor RTD behaviour for various future applications such as tunable THz communications, 5G/6G technology, and physically unclonable functions (PUF) generation.
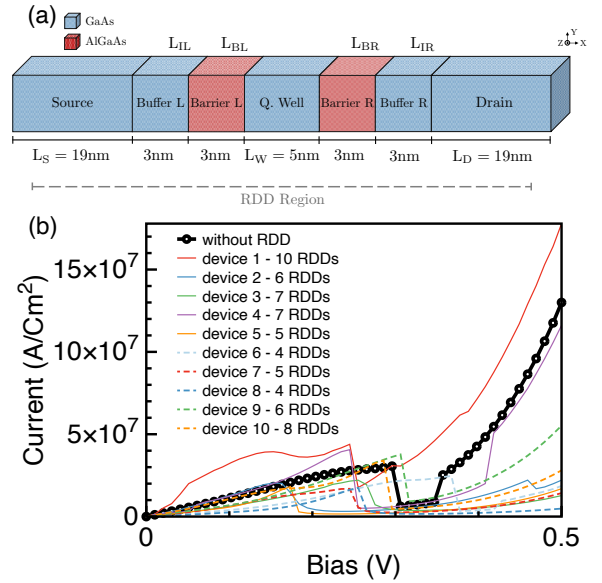

Fig. 5. (a) The schematic illustration of the double barrier RTD device with a 10nm$\times$10nm square cross-section and the total length of 55nm. (b) The current-voltage (I-V) characteristics of 10 RTD configurations with RDDs distributed within the RDD region highlighted in (a) - 3nm from each end. The baseline structure without any RDDs (smooth device) is presented in black for comparison purposes. It can be seen that devices with the same number of dopants, e.g., No. 6 vs No. 8, No. 5 vs No. 7, No. 2 vs No. 9, and device No. 3 vs No. 4, have a huge variation of the resonance peak.

C. Mobility Calculation for Nanowires

Using the KG module, we have evaluated the scattering rates and the phonon-limited electron mobility for Si NWTs for the <110> transport direction considering different widths (ranging from 3nm to 6nm) and shapes (square, cylindrical and elliptical) and acoustic and optical phonon scattering mechanisms.

Figure 6(a) shows the acoustic and optical phonon scattering rates for the 3nm and 6nm circular NWTs. The scattering

rate peaks are nearer for the 6nm device compared to the 3nm one because they represent the subband levels. When the mechanisms are compared, the acoustic phonon has higher scattering rates than the optical one for lower energy which limits the electron mobility (Figure 6(b)), as the mobility is inversely proportional to the scattering rate following the KG formula. Finally, Figure 6(c) shows the phonon-limited electron mobility as a function of the device width (major diameter for the elliptic shape) for a given line density. Two different results can be extracted from this figure: (1) the reduction of the electron mobility when the devices are shrinking down, and (2) the higher performance of the elliptic NWT [12].
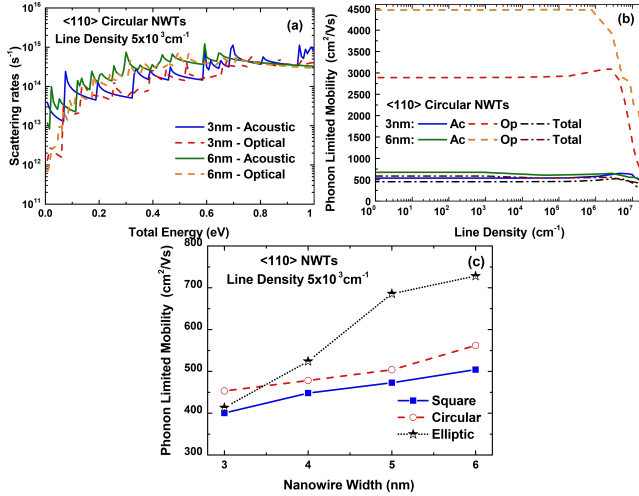

Fig. 6. Results simulated using the Kubo-Greenwood module of NESS for different NWTs considering the <110> transport direction: (a) Acoustic and optical phonon scattering rates considering all the subbands and valleys as a function of the total energy considering for 3nm and 6nm circular NWTs with a line density of 5×10^{11}cm^{-2}. (b) Phonon-limited electron mobility as a function of the line density considering the acoustic (Ac), optical (Op), and total phonon-limited mobility for 3nm and 6nm circular NWTs. (c) Phonon-limited electron mobility as a function of the NWT width (major diameter for the elliptic case) considering the square, circular, and elliptic NWT shapes with a line density of 5×10^{11}cm^{-2}. Note that the ratio between the major and minor axes for the elliptic shape is 1.5.

D. Resistive Memory Devices

In previous works [13], [14] we have demonstrated that the Kinetic Monte Carlo (KMC) module is a powerful tool to help investigate the characteristics of flash memory devices. One of these promising candidates is the polyoxometalate (POM) molecule-based cell. Theses device owe their advantage to their small size, redox properties (limit device variability) and compatibility with the CMOS fabrication process [13], [14]. Device simulation using the KMC method allowed to study device characteristics, like retention time. It was shown that a retention time of 10^{15} s can be achieved that corresponds to the industry standard of 10 years [13]. However, it was also shown that device retention time variability could be a limiting factor, therefore further optimization is required in which case the KMC module of NESS can aid the design [14].

Another promising contender for memory devices is the resistive random-access memory (RRAM). The KMC is used to account for ionic and electronic transport through the master equations as in Ref. [15]. In Fig. 7 the RRAM behaviour is shown, the forming process and the operation of write (Set phase) and erase (Reset phase) processes.
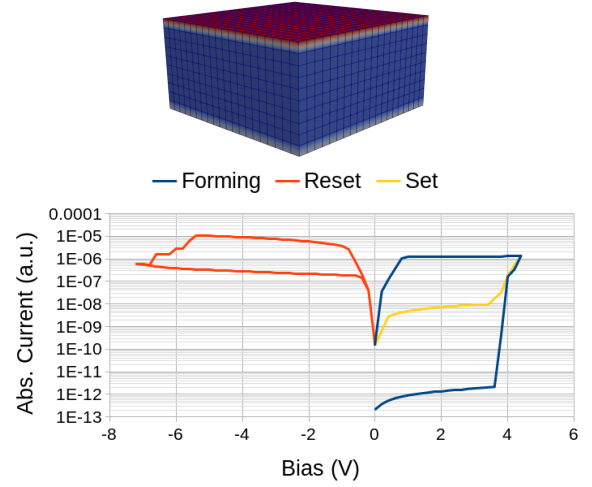

Fig. 7. (top) RRAM device schematics, insulator is sandwiched between two metal contacts. (bottom) Simulation characteristic of a bipolar RRAM device.

V. CONCLUSION

In this paper we have presented an overview of our flexible and modular TCAD software NESS. We have summarised the workings of its different modules, and how they are linked. Furthermore, we have demonstrated the capabilities of this tool by presenting demonstrative results obtained by simulating state-of-the-art and emerging devices.

VI. ACKNOWLEDGMENT

REFERENCES

[1] NESS. [http://web.eng.gla.ac.uk/groups/devmod/index.php/software/]
[2] S. Berrada *et al.*, *International Conference on Simulation of Semiconductor Processes and Devices (SISPAD)*, Sep. 2018, pp. 22–25.
[3] S. Berrada *et al.*, *J. Comput. Electron.*, vol. 19, pp. 1031–1046, 2020.
[4] C. Medina-Bailon *et al.*, *J. Microelectronic Manufacturing*, vol. 3, no. 4, pp. 20030404, 2020.
[5] C. Medina-Bailon *et al.*, *Micromachines*, vol. 12, no. 6, pp. 680, 2021.
[6] O. Badami *et al.*, *Applied Sciences*, vol. 9, no. 9, p. 1895, 2019.
[7] Atomistix ToolKit, QuantumWise A/S. [www.quantumwise.com]
[8] T. Dutta *et al.*, *14th IEEE Nanotechnology Materials and Devices Conference (NMDC)*, 2019, pp. 1–4.
[9] M. Ancona, *J. Comp. Electron.*, vol. 10, no. 1, pp. 65–97, 2011.
[10] M. Luisier *et al.*, *Phys. Rev. B*, vol. 80, p. 155430, Oct 2009.
[11] T. Sadi *et al.*, *Materials*, vol. 12, no. 1, p. 124, 2019.
[12] C. Medina-Bailon *et al.*, *IEEE Electron Device Letters*, vol. 40, no. 10, pp. 1571 – 1574, 2019.
[13] P. Lapham *et al.*, *International Conference on Simulation of Semiconductor Processes and Devices (SISPAD)*, 2020, pp. 273–276.
[14] J. Ding *et al.*, *Semiconductor Science and Technology*, vol. 36, no. 7, pp. 075021, jun 2021.
[15] C. Medina-Bailon *et al.*, *International Conference on Simulation of Semiconductor Processes and Devices (SISPAD)*, 2020, pp. 293–296.